



UNICA

UNIVERSITÀ
DEGLI STUDI
DI CAGLIARI



Università di Cagliari

UNICA IRIS Institutional Research Information System

This is the Author's pre-print version of the following contribution:

SABA, Luca

[INTERNATIONAL JOURNAL OF NEUROSCIENCE](#)

SBM vs VBM for highlighting similarities and differences between chronotype and Parkinson's MRI scans: a preliminary analysis

The publisher's version is available at:

Codice DOI

<https://dx.doi.org/10.1080/00207454.2023.2292958>

When citing, please refer to the published version

Pre-print version

SBM vs VBM for highlighting similarities and differences between Chronotype and Parkinson's MRI scans: a preliminary analysis

Sebastiano Vacca¹, Jasjit S Suri², Luca Saba³

¹University of Cagliari, School of Medicine and Surgery, Cagliari, Italy

²Stroke Diagnostic and Monitoring Division, AtheroPoint™, United States and Advanced Knowledge Engineering Centre, Global Biomedical Technologies Inc. (GBTI), Roseville, CA, United States.

³Department of Radiology, Azienda Ospedaliero-Universitaria (A.O.U.), di Cagliari—Polo di Monserrato, Cagliari, Italy.

Corresponding Author: Sebastiano Vacca, University of Cagliari, Faculty of Medicine and Surgery, Cagliari, Italy. Email: sebastianovacca@hotmail.it

Abstract

Introduction: Voxel-Based Morphometry (VBM) and Source-Based Morphometry (SBM) are two widely used techniques for analyzing structural Magnetic Resonance Imaging (MRI) data of the brain. While VBM is a voxel-wise approach that compares differences in gray and white matter volume, density, or concentration between groups or conditions, SBM identifies patterns of structural variation across the whole brain using independent component analysis (ICA). The purpose of this study is to compare the performance of VBM and SBM in detecting differences in brain structure.

Methods: Source-Based-Morphometry through the Fusion Ica Toolbox, and Voxel-Based-Morphometry, with the CAT12 pipeline, were used to test differences and similarities in Parkinson's patients MRI scans and Chronotypes in 33 subjects divided into three groups: a Parkinson's Group (PG), an Early Chronotype Group (EG), and a Late Chronotype Group (LG) (with each group consisting of 11 subjects). Circadian preference, daytime sleepiness and sleep quality were tested, while MRI data were acquired with a 3T scanner.

Results: The average age for the EG was 32.1 years old; for the LG it was 30.3 years old; for the PG it was 38.6 years old. SBM statistics showed several clusters surviving the analysis and the conversion to z-map score with a threshold of $z > 2$. Multiple Regions of Interest (ROI) were identified as different between the groups and the components with the lowest p value (< 0.05) were the 1st one for the PG-EG and the 4th one for the PG-LG analysis. In the Talairach Coordinates analysis, the Middle Frontal Gyrus and the Lentiform Nucleus were identified as denser in GMV or WMV.

Conclusion: Our study highlights the importance of choosing the appropriate method for analyzing structural MRI data. While VBM is a powerful technique for identifying local differences in brain structure, SBM provides a more comprehensive view of brain structural variation and can reveal patterns that are not detectable by VBM. Future studies should consider using both VBM and SBM to fully characterize brain structural differences in various clinical and cognitive populations.

List of Abbreviations:

MRI: Magnetic Resonance Imaging

SBM: Source-Based-Morphometry

jSBM: joint-Source-Based-Morphometry

VBM: Voxel-Based-Morphometry

PD: Parkinson's Disease

EC: Early Chronotype

LC: Late Chronotype

PG: Parkinson's Disease Group

EG: Early Chronotype Group

LG: Late Chronotype Group

PCA: Principal Component Analysis

ICA: Independent Component Analysis

GMV: Grey Matter Volume

WMV: White Matter Volume

FWE: Family Wiser Error

MDL: Minimum Description Length

CAT12: Computational Anatomy Toolbox

SPM12: Statistical Parameter Mapping

FIT: Fusion ICA Toolbox

jICA: joint Independent Component Analysis

HC: Healthy Controls

Introduction

Neuroimaging analysis is a critical tool for understanding the structural and functional changes of the brain. Structural Magnetic Resonance Imaging (sMRI) data can be analyzed using different techniques, which vary in their sensitivity, specificity, and ability to identify patterns of structural variation across the whole brain.

Two commonly used MRI data analysis methods in detecting structural variations in the brain are the Voxel-Based-Morphometry (VBM) [1] and the Source-Based-Morphometry (SBM) [2-3]. VBM is an automated technique that uses statistics to identify differences in brain anatomy between groups of subjects, which can be used to infer the presence of atrophy or tissue expansion in subjects with disease [1, 4-6]. It typically uses T1-weighted volumetric Magnetic resonance imaging (MRI) scans and essentially performs statistical tests across all voxels in the image to identify volume differences between groups. As such, VBM is a powerful tool for assessing structural changes in the brain that can help increase understanding of disease processes.

SBM is a data-driven linear multivariate approach for decomposing structural brain imaging data into commonly covarying imaging components and subject-specific loading parameters [2-3]. SBM is an extension of VBM and includes independent component analysis (ICA). In contrast to univariate analysis, which examines each voxel in isolation, SBM considers the relationships between voxels and identifies patterns of covariation across the entire brain: this allows for the identification of complex and weak effects from high-dimensional datasets while simultaneously performing data reduction procedures. The imaging data can be reduced from 20,000 voxels to a handful of networks or patterns, which can then be examined for group differences or other effects. Overall, SBM provides a more comprehensive and nuanced approach to analyzing structural brain imaging data compared to traditional univariate methods. [7-11]. More in detail, joint-SBM (jSBM), uses joint-ICA (jICA) to break down processed images of brain tissue into shared components and statistical analysis by identifying patterns of activity that are common to both types of data, finding the significant shared components that differ between groups. These shared components are combinations of connected brain regions that vary together among subjects. [3,11].

Both VBM and SBM have been used to look into a variety of psychiatric diseases and neurological illnesses, such as Schizophrenia, Major Depressive Disorder, Multiple Sclerosis and Bipolar Disorder [8-10] but, to our

knowledge no direct comparison of their efficacy in Parkinson Disease (PD) and Chronotype has been explored.

Circadian rhythms are daily oscillations found in most aspects of human physiology, from early development to the latest stages of life [12]. Their role is crucial in regulating all aspects of our existence, and that is why they are constantly under the spotlight as a primary or secondary cause of a plethora of diseases [13]. The link between different chronotypes, their disruption, and neurodegenerative disorders has been investigated in the past years, leading to an increasing amount of evidence pointing to a bidirectional correlation [14, 15, 12]. Some authors have suggested that varying in the circadian clock, could lead to the prevention and improvement of neurodegenerative diseases [14]. Amongst these, one of the most famous for having a correlation with sleep disorders, which in turn leads to circadian alteration, is PD [16, 17].

Parkinson's is a neurodegenerative disorder that involves the progressive loss of dopaminergic neurons in the substantia nigra and cortical atrophy [18]. One of PD's prodromal symptoms, which relinquishes even after its initial phase, is REM sleep disorder [19], which can be helpful in the diagnosis of PD early on. Besides that, excessive daytime sleepiness [16] has been associated with PD, together with other nocturnal sleep alterations, such as restless leg syndrome and sleep apnea. All these manifestations are going to affect patients' internal clock and can even contribute to the process of neuronal degeneration, as mentioned before [15]. As cited earlier there are also concerns and hypotheses on a correlation on the other way around, and that is why there've been questions regarding Chronotypes disruption and PD, but with conflicting results [20].

The purpose of this paper is to compare the outcomes of each method and assess the effectiveness of VBM and SBM in detecting structural brain differences in individuals with PD and healthy controls. We will investigate whether one technique is better suited than the other to detect anatomical variations and determine which method is more efficient in identifying group differences. By comparing VBM and SBM results, we hope to contribute to the growing literature on neuroimaging techniques and their application in clinical settings.

Methods

The study population consisted of 33 subjects divided into three groups: a Parkinson's Group (PG), an Early Chronotype Group (EG), and a Late Chronotype Group (LG). Each group consisted of 11 subjects. The PG group included patients data and scans downloaded from The Parkinson Progression Marker Initiative (PPMI)[21], while the EG and LG data has been acquired from [<https://openneuro.org/datasets/ds003826/versions/3.0.1> dataset]. Regarding the LG and EG the data was obtained as follows [22]:

Circadian preference and the subjective amplitude of the circadian rhythms for each participant were assessed using the Chronotype Questionnaire (ChQ) [23, 24] whereas daytime sleepiness and sleep quality was tested with, respectively, Epworth Sleepiness Scale (ESS) [25] and Pittsburgh Sleep Quality Index (PSQI) [26]. All the questionnaire measurements were collected before acquiring the brain imaging data.

MRI data were acquired with a 3T scanner (Magnetom Skyra, Siemens) using a 20-channel or 64-channel head/neck coil. The high-resolution structural brain images were collected with a T1 MPRAGE sequence (176 sagittal slices; $1 \times 1 \times 1.1$ mm³ voxel size; TR = 2300 ms, TE = 2.98 ms, flip angle = 9, GRAPPA acceleration factor 2)

Meanwhile, the PG MRI data selected was acquired with a 3T scanner (Siemens). The high resolution structural brain images were collected with a magnetization-prepared rapid gradient-echo (3D T1 MPRAGE) sequence ($1 \times 1 \times 1.1$ mm³ voxel size; TR = 2300 ms, TE = 3 ms, flip angle = 9, GRAPPA acceleration factor 1 or 2).

Voxel-Based-Morphometry Steps

Preprocessing: The MRI scans are preprocessed to correct for image distortions, intensity non-uniformities, and spatial normalization to a standard template. The data were analyzed using CAT12

(<http://www.neuro.uni-jena.de/cat/>; CAT12, version r1109) implemented in SPM12

(<https://www.fil.ion.ucl.ac.uk/spm/software/spm12/>). Data processing for grey matter volume (GMV) and white matter volume (WMV) included spatial normalization, segmentation, and smoothing (6 mm full-width

half-maximum Gaussian kernel) to increase the signal-to-noise ratio and account for individual differences in brain anatomy. . The new segmentation algorithm implemented in SPM12 was used to segment the T1-weighted structural images into gray matter, white matter, and cerebrospinal fluid.

Statistical analysis: To compare the variations in GMV between the groups, two VBM analyses were carried out. In analysis 1, PG and LG were contrasted; in analysis 2, EG and PG were. The entire brain volume (the sum of GMV and WMV) of each brain was utilized as a covariant to adjust for any notable disparities between the brains. The volume of the brain was calculated using the toolbox tissue volume in SPM12.

Under the option Masking, which replicates which voxel is included in the analysis, any voxel with a value of 0 (implicit masking) or a value below 0.01 (threshold masking with an absolute threshold of 0.01) was excluded from the study [27]. The other parameters in this phase were implemented as necessary. The Estimate option had the traditional technique set, which involves running the analysis multiple times. One t-contrast was established as -1 1 to display the t-statistics results. Additionally, an FWE (family-wise error correction) with a p-value of 0.05 was utilized to limit the likelihood of false positives.

Source-Based-Morphometry Steps

Preprocessing of structural MRI data, including skull stripping, spatial normalization, and segmentation into gray matter, white matter, and cerebrospinal fluid, as seen earlier. Creation of a group-level covariance matrix based on the gray matter images of all subjects in the study. Decomposition of the covariance matrix using independent component analysis (ICA) to identify maximally spatially independent sources exhibiting covariation among subjects in structural gray matter MRI images.

Identification of structural magnetic resonance imaging (sMRI) differences between groups by comparing the subject-specific loading coefficients for each component between groups. This methodology allows for the identification of complex and weak effects from high-dimensional datasets while simultaneously performing data reduction procedures.

Two SBM studies between PG and EG and PG and LG were conducted by using the Fusion ICA Toolbox (FIT; version 2.0e; <https://trendscenter.org/software/fit/>), individual whole-brain maps of GMV and WMV were entered into a joint-ICA (jICA) [3, 28]. The minimum description length was used to estimate the

number of components for each modality (MDL). For each modality, eight components were discovered. To pre-select components of possible relevance, the results of (two-tailed) two-sample t-tests on the loading parameters of PG, EG, and LG as implemented in FIT were used. A threshold of $p < 0.05$ was considered statistically significant.

Results

General Results

Each group consisted of 11 subjects. The average age for the EG was 32.1 years old; for the LG it was 30.3 years old; for the PG it was 38.6 years old. In the PG 7 males and 4 females were analyzed, while in the EG 5 males and 6 females, and in the LG 4 males and 7 females.

Voxel-Based-Morphometry

By applying a Family Wise Error (FWE) correction for multiple comparisons (p -value < 0.05), no voxels survive the difference analysis between PG and EG with tissue map computed with CAT12 and then visualized with xjview. When comparing PG to LG, the difference analysis resulted in some surviving voxels in the left and right putamen, as seen in figure 1.

Source-Based-Morphometry

The results of the SBM statistics obtained through the jointICA with GMV and WMV showed several clusters surviving the analysis and the conversion to z-map score with a threshold of $z > 2$. Multiple Regions of Interest (ROI) were identified as different between the groups, as can be seen in figures 1 through 4, both at cortical and subcortical level. We then analyzed the mixing matrix using a two-sample t -test for patients versus controls. The components with the lowest p value (< 0.05) were the 1st one for the PG-EG and the 4th one for the PG-LG analysis.

In the Talairach Coordinates analysis, table 1-2, we can see that cortical region like the Middle Frontal Gyrus or subcortical like the Lentiform Nucleus, were identified as denser in GMV or WMV, in EG and LG compared to PG, but depending on the feature (GMV or WMV) the same areas resulted as with fewer

voxels (p value of < 0.05). The differences in positive mean that there is a denser cluster, and by looking at the volume and the random effects one of the two groups, we can determine if one has more of these cluster than the other. In this case, the EG resulted having fewer of these groups of voxels, while the LG was more different from the PG.

Discussion

The purpose of this study was to investigate the effectiveness of two methods, Voxel-Based Morphometry and Surface-Based Morphometry in identifying differences in brain MRI scans between individuals with early onset Parkinson's disease, early chronotype subjects, and late chronotype subjects. VBM has been widely used for decades to analyze MRI scans, while SBM has recently emerged as a more accurate and informative alternative. Through this study, we aimed to determine whether SBM would be more effective than VBM in identifying differences in brain MRI scans between the three groups.

The correlation between chronotype and neurodegenerative disorders has been steadily gaining more attention; amidst the studies conducted, Culell et al. [29] investigated chronotype, sleep efficiency and sleepiness correlations while considering several neurodegenerative disorders, such as PD, Multiple Sclerosis and Alzheimer's disease. Their research made use of a Mendelian Randomization (MR) study with two samples, while choosing 12 sleep-related variables based on Genome-Wide Association Study (GWAS) data. Through this approach they were able to discover multiple associations, as morning chronotype and insomnia were positively correlated with later PD age of onset, pointing out that an evening chronotype might lead to an earlier PD age of onset ($b = 1.07$ ($se = 0.37$)). On the other hand, Videnovic et al. [17] research, where 20 patients with Parkinson's disease getting stable dopaminergic treatment and 15 age-matched controls participated in a cross-sectional study, did not lead to any correlation between Parkinson features and chronotype. In contrast to both studies, Tarianyk et al. [20] after examination of 64 patients with various PD motor subtypes, documented a higher percentage of Parkinson's Disease patients with a tendency towards an evening chronotype, established according to the Munich Chronotype Questionnaire. On a different note, Marano et al. [30] findings support the inverse: after investigating 50 PD patients with the Morningness Eveningness Questionnaire and monitoring them with a motion sensor, they demonstrated

that axial motor dysfunction, the existence of motor fluctuations, and quality of life were different (p value = 0.05), with a propensity towards a morning chronotype, especially a late morning one; moreover, a morning, or intermediate, chronotype were associated with motor and non-motor signs of a worse disease phenotype with visuospatial cognitive dysfunctions [30].

These findings show how despite numerous efforts and high-quality scientific results, there has not been a consensus on the association between PD and a chronotype. Furthermore, all the previous literature did not focus on MRI analysis, and the studies focusing on the comparison between SBM and VBM did not take into consideration Parkinson Disease and chronotypes. Thus, our research points at adding on both fields, more on the superiority of SBM versus VBM, due to the limitations of the data.

Indeed, our findings suggest that SBM is more effective than VBM in identifying the nuances of the MRI scans and providing more detailed insights into the differences between the groups.

In terms of VBM analysis, no significant differences were found between the PG and EG groups. However, when comparing the PG group to the LG group, we found several voxels in the left and right putamen that survived the multiple comparison correction. These findings are in accordance with the typical findings in MRI's scans of Parkinson, as in the review by Pagano et al [31], where they have reported the findings of a Righini et al. [32] research. Righini et al. documented that putaminal T2 hypointensity was observed in 27 patients with PD. On the other hand, Ramírez et al. [33] conducted a VBM study by investigating any differences in the gray and white matter morphology between 144 de novo PD patients and 66 controls from the PPMI database, while comparing two pipelines' results, such as CAT12 and VolBrain; their results did not lead to any statistically significant findings regarding any differences between the PD and healthy controls, suggesting that VBM might not be suited for this kind of analysis.

To the best of our knowledge, no study has previously investigated the differences between healthy controls and PD patients by conducting a SBM analysis. Our SBM research revealed several clusters that survived the joint independent component analysis with grey matter volume and white matter volume. Multiple regions of interest were identified as being statistically different between the groups at both cortical and subcortical levels. In particular, the PG-EG comparison showed that the 1st component had the lowest p -value, while the PG-LG comparison showed that the 4th component had the lowest p -value. These results

suggest that different brain regions may be affected in different ways depending on the specific comparison being made.

As cited earlier, usually structural MRI is not regarded as valid method for differentiating between PD and HC [34], and the areas that are mostly identified as atrophied in PD are the ones that usually stand out while looking at MRIs, like the putamen or the amygdala [34, 35]. In our evaluation, the putamen was among the areas that contributed the most in distinguishing between PG and HC, but also cortical areas were among the ones most affected by it. This result goes against some of the previous evidence, such as in the study by Blair et al. [35], where no neocortical areas were found to be statistically different between PD and HC, after a VBM analysis that comprehended 103 HC and 136 PD patients. In the same study, there were some subcortical areas found to have a lower GMV, as basal forebrain, amygdala, and entorhinal cortex. In contrast, Long et al. [36] in a VBM and resting-state function MRI study, highlighted differences in both analysis, while examining 19 early PD patients and 27 HC. In particular, the VBM analysis showed brain regions, which has been selected as features more than 23 times, as statistically different between the two groups regarding the GM, such as the paracentral lobule, and precentral gyrus; while for WM, the middle and frontal gyrus, Rolandic operculum, the olfactory cortex and the precentral gyrus were significantly different.

In our SBM evaluation, the cortical brain regions identified as statistically different, with a higher or lower GMV and WMV, were several. Amongst those, we have found the superior frontal gyrus, which is involved in self-awareness and executive functions, or the medial frontal gyrus that is associated with high-level executive functions and decision-related processes. One of the most relevant regions identified by the SBM technique, was a sub-gyral one, composed of the areas 6,7,8,20,31,37,39 and 40, where difference between PG and LG was the largest of any other region. Amongst these areas, we find relevant neuronal population for movement and its planning, moreover, the fusiform, angular and supramarginal gyri, involved in complex function and tasks, as calculus and face recognition.

These results show how the SBM was able not only to reproduce the VBM ones, such as identifying the putamen as a key area for differentiating between PD and HC, but went further into detail, successfully pointing out subcortical and cortical areas that might differ between the groups, providing more information

in respect to the previous literature on VBM as well. Furthermore, it allowed us to differentiate between the LC and EC when comparing them to the PG. This is concordant with previous studies conducted, where SBM has been compared to VBM for a more specific and detailed characterization of neurodegenerative and psychiatric disorders [5,7,2]. In particular, Singh et al. [5], provided an excellent example of SBM's superiority on VBM. By studying 20 children affected by bipolar disorder, they demonstrated how VBM did not reveal any increase in GMV and WMV, while SBM was able to demonstrate it in the bilateral angular gyrus, bilateral inferior temporal, left supplementary motor area and left middle temporal region. Accordingly, Bergsland et al. [7] evaluated 152 patients diagnosed with Multiple Sclerosis at baseline and at a 10-year follow-up period, utilizing a longitudinal SBM analysis. Their results, statistically significant as with a p-value < 0.05 , showed how SBM was optimal in characterizing GM atrophy in areas associated with motor and cognitive functioning. Lastly, Xu et al. [37] compared VBM and SBM pipelines on 120 HC and 120 schizophrenic patients. Their SBM approach showed higher accuracy and details, as it was able to spot GM alterations not identified by VBM in the basal ganglia, the parietal, and the occipital lobe.

It is important to note that the limitations of our study. First, the sample size was relatively small: we tried to limit false positives in the VBM analysis, as suggested by Scarpazza et al. [38], while equally distributing the subjects, this limitation should be considered when interpreting the results and these results could be considered preliminary analysis. The second limitation is the relative unbalance between sexes in the groups can be a concern regarding the analysis validity. Third, the retrospective nature of the analysis and the difference in age between the groups may have influenced the outcomes of the study. Despite these limitations, our preliminary findings suggest that SBM is a more effective method than VBM for identifying differences in brain MRI scans, particularly in identifying their nuances and providing more detailed insights into the differences between groups. Further studies, with larger sample sizes and more balanced genders, are needed to confirm our findings.

Conclusions

In this study, we compared the accuracy of two neuroimaging techniques, VBM and SBM, to identify differences in brain MRI scans between groups of Parkinson's Disease patients, Early Chronotype subjects,

and Late Chronotype subjects. Our findings suggest that SBM is a more accurate technique for identifying these differences and provides more nuanced insights than VBM. Specifically, we found that SBM was able to identify more regions of interest and provided greater detail on the differences between the groups. While both techniques were consistent with their results, SBM has been proven to be more accurate and provide more information than VBM. These findings have implications for future studies investigating the superiority of SBM in regard to VBM in analyzing MRI from patients affected by neurodegenerative disorders.

TABLES LEGENDS

Table 1

Voxels above the threshold of $Z > 2$ were converted from Montreal Neurological Institute (MNI) coordinates to Talairach coordinates and entered a database to provide anatomic and functional labels for the left (L) and right (R) hemispheres. The volume of voxels in each area is provided in cubic centimeters (cc). Within each area, the maximum Z value and its coordinate are provided.

Table 2

Voxels above the threshold of $Z > 2$ were converted from Montreal Neurological Institute (MNI) coordinates to Talairach coordinates and entered a database to provide anatomic and functional labels for the left (L) and right (R) hemispheres. The volume of voxels in each area is provided in cubic centimeters (cc). Within each area, the maximum Z value and its coordinate are provided.

TABLES

Table 1

Talairach Table of sMRI Components of Interest			
Area	Brodmann Area	volume (cc)	random effects: Max Value (x, y, z)
PG-LG			
IC4 Positive - Feature 1			
Middle Frontal Gyrus	6, 8, 9, 10, 11, 46	9.9/9.0	6.5 (-43, 29, 18)/9.4 (34, -2, 46)
Sub-Gyral	*	0.8/1.2	8.7 (-1, -79, -29)/8.1 (3, -79, -29)
Uvula	6, 30, 40	6.8/3.1	8.7 (-13, -52, 58)/5.7 (50, -19, 20)
Pyramis	*	1.7/1.2	5.9 (-7, -79, -34)/7.4 (6, -79, -31)
Superior Parietal Lobule	*	2.1/1.3	7.1 (-4, -79, -26)/6.4 (6, -76, -29)
IC4 Positive - Feature 2			
Sub-Gyral	6, 7, 8, 20, 31, 37, 39, 40	55.8/50.5	4.6 (-27, 10, 22)/4.7 (30, -40, 46)
Middle Occipital Gyrus		19 3.1/2.0	4.6 (-33, -73, 17)/3.6 (33, -74, 13)
Middle Frontal Gyrus	6, 8, 9, 10, 11, 46, 47	8.1/7.0	4.5 (-27, 42, -5)/4.3 (25, 45, -5)

Table 2

Talairach Table of sMRI Components of Interest

Area	Brodmann Area	volume (cc)	random effects: Max Value (x, y, z)
PG-EG			
IC1 Positive - Feature 1			
Lentiform Nucleus	*	6.5/3.7	9.1 (-28, -6, 4)/7.0 (30, -10, 2)
Extra-Nuclear		13 8.4/4.0	7.6 (-31, -12, -1)/6.3 (33, -10, -1)
Precuneus	7, 19, 31	4.0/5.1	6.7 (-25, -64, 40)/5.1 (30, -59, 39)
Sub-Gyral		20 6.1/5.1	6.7 (-18, -68, -10)/4.8 (33, -59, 42)
Culmen	*	5.2/6.8	4.9 (-15, -63, -7)/6.6 (15, -48, -8)
IC1 Positive - Feature 2			
Middle Frontal Gyrus	6, 8, 9, 10, 11, 46, 47	6.7/5.4	6.7 (-18, -1, 58)/9.7 (33, 25, 40)
Medial Frontal Gyrus	4, 6, 8, 9, 10, 32	4.0/2.7	8.8 (-10, 0, 58)/6.4 (21, 11, 45)
Postcentral Gyrus	2, 3, 5, 7, 40, 43	5.4/2.9	5.3 (-55, -22, 33)/8.3 (50, -16, 38)
Lingual Gyrus	17, 18, 19, 30	2.3/5.6	5.0 (-19, -66, -3)/7.9 (15, -58, 4)

Figure 1: VBM Analysis – Late Chronotype

Differences in grey matter concentration between Late Chronotype and Parkinson delineated by VBM

Figure 2: SBM - Early Chronotype Grey Matter

Differences in grey matter concentration between Early Chronotype and Parkinson delineated by SBM. The voxels above the threshold of $Z > 2$ are shown.

Figure 3: SBM - Early Chronotype White Matter

Differences in white matter concentration between Early Chronotype and Parkinson delineated by SBM. The voxels above the threshold of $Z > 2$ are shown

Figure 4: SBM - Late Chronotype Grey Matter

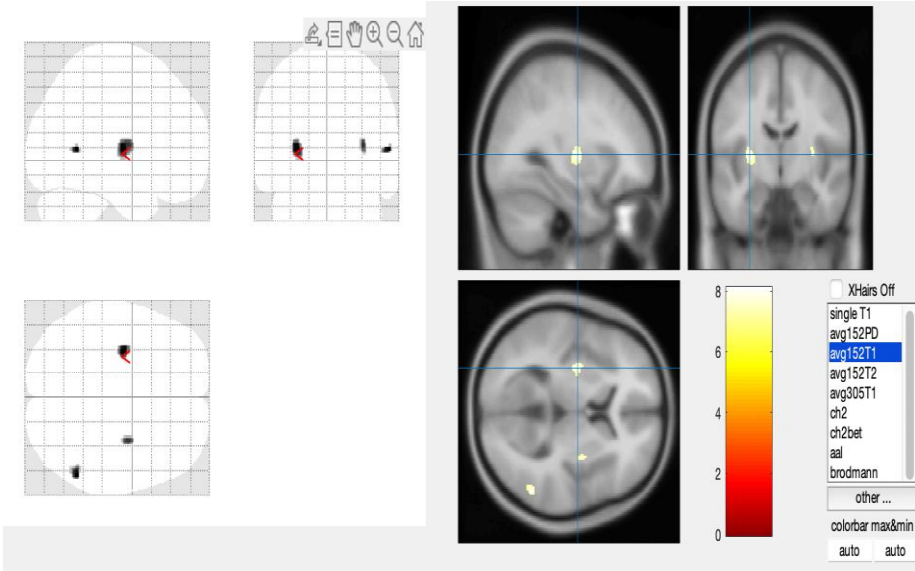
Differences in grey matter concentration between Late Chronotype and Parkinson delineated by SBM. The voxels above the threshold of $Z > 2$ are shown.

Figure 5: SBM - Late Chronotype White Matter

Differences in white matter concentration between Late Chronotype and Parkinson delineated by SBM. The voxels above the threshold of $Z > 2$ are shown.

FIGURES

Figure 1



// Left Cerebrum // Sub-lobar // Lentiform Nucleus // Gray Matter // Putamen // Putamen_L (aal3v1)

Figure 2

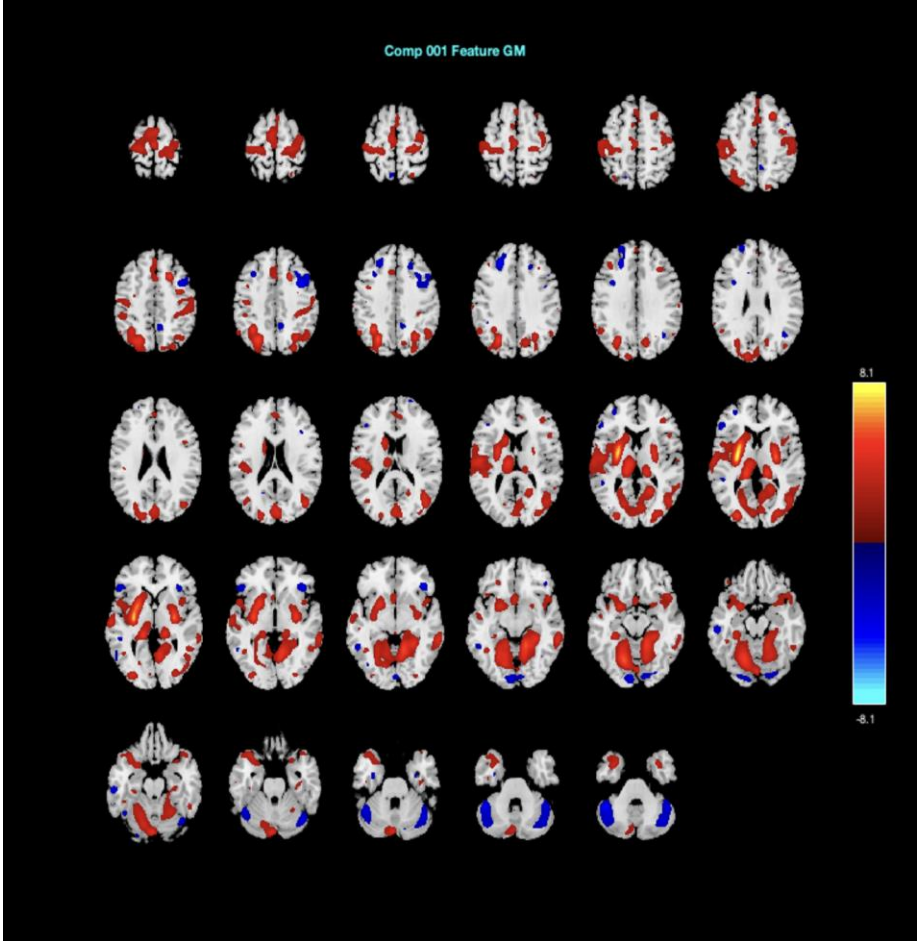


Figure 3

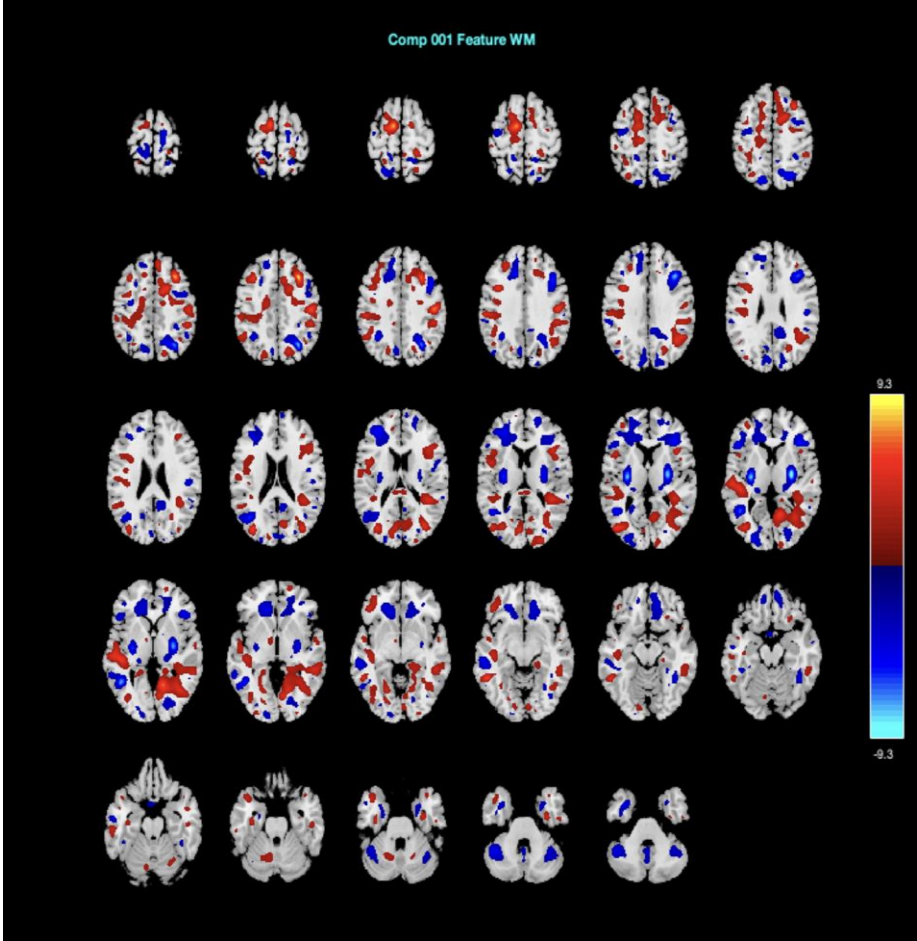


Figure 4

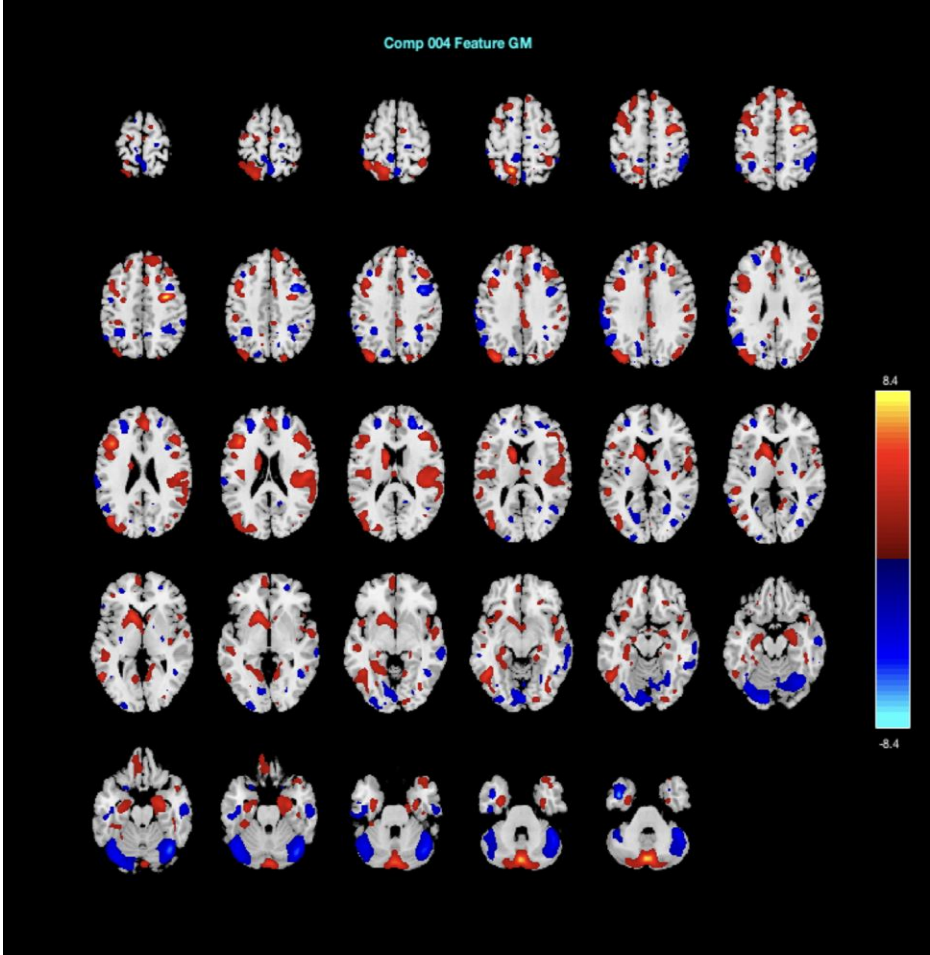
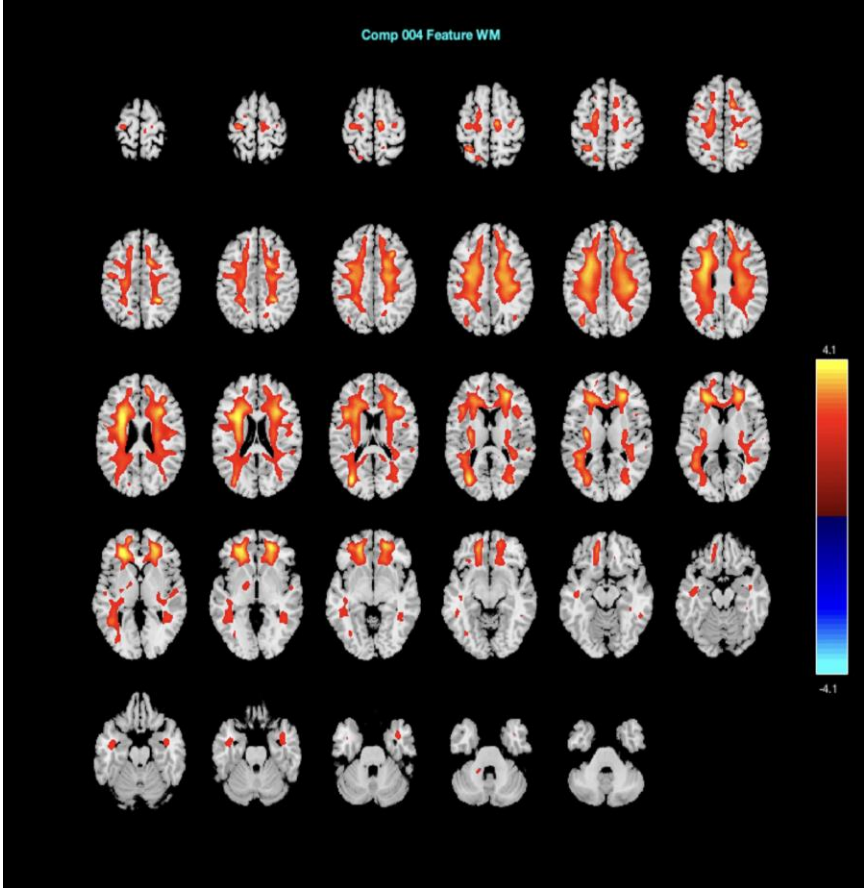


Figure 5



References

1. Voxel-Based Morphometry: An Automated Technique for Assessing Structural Changes in the Brain
Jennifer L. Whitwell *Journal of Neuroscience* 5 August 2009, 29 (31) 9661-9664.
2. Gupta, C.N., Turner, J.A. & Calhoun, V.D. Source-based morphometry: a decade of covarying structural brain patterns. *Brain Struct Funct* 224, 3031–3044 (2019).
3. Xu L, Pearlson G, Calhoun VD. Joint source based morphometry identifies linked gray and white matter group differences. *NeuroImage*. 2009;44(3):777-789.
4. Nemoto K. *Brain Nerve*. 2017;69(5):505-511. doi:10.11477/mf.1416200776
5. Ashburner J, Friston KJ. Voxel-Based Morphometry—The Methods. *NeuroImage*. 2000;11(6):805-821. doi:https://doi.org/10.1006/nimg.2000.0582
6. Mechelli A, Price C, Friston K, Ashburner J. Voxel-Based Morphometry of the Human Brain: Methods and Applications. *Current Medical Imaging Reviews*. 2005;1(2):105-113. doi:https://doi.org/10.2174/1573405054038726
7. Xu, L., Groth, K.M., Pearlson, G., Schretlen, D.J. and Calhoun, V.D. (2009), Source-based morphometry: The use of independent component analysis to identify gray matter differences with application to schizophrenia. *Hum. Brain Mapp.*, 30: 711-724. https://doi.org/10.1002/hbm.20540
8. Singh, A., Arya, A., Agarwal, V. *et al.* Grey and white matter alteration in euthymic children with bipolar disorder: a combined source-based morphometry (SBM) and voxel-based morphometry (VBM) study. *Brain Imaging and Behavior* 16, 22–30 (2022). https://doi.org/10.1007/s11682-021-00473-0
9. Wang KC, Hu YF, Yan CG, et al. Brain structural abnormalities in adult major depressive disorder revealed by voxel- and source-based morphometry: evidence from the REST-meta-MDD Consortium. *Psychological Medicine*. 2022:1-11. doi:10.1017/S0033291722000320
10. Bergsland N, Horakova D, Dwyer MG, et al. Gray matter atrophy patterns in multiple sclerosis: A 10-year source-based morphometry study. *NeuroImage: Clinical*. 2018;17:444-451.
11. Moosmann M, Eichele T, Nordby H, Hugdahl K, Calhoun VD. Joint independent component analysis for simultaneous EEG-fMRI: principle and simulation [published correction appears in *Int J*

Psychophysiol. 2008 Apr;68(1):81]. *Int J Psychophysiol.* 2008;67(3):212-221.

doi:10.1016/j.ijpsycho.2007.05.016

12. Logan, R.W., McClung, C.A. Rhythms of life: circadian disruption and brain disorders across the lifespan. *Nat Rev Neurosci* 20, 49–65 (2019)
13. Knutson KL, von Schantz M. Associations between chronotype, morbidity and mortality in the UK Biobank cohort. *Chronobiol Int.* 2018;35(8):1045-1053
14. Leng Y, Musiek ES, Hu K, Cappuccio FP, Yaffe K. Association between circadian rhythms and neurodegenerative diseases. *Lancet Neurol.* 2019;18(3):307-318
15. Werdann M, Zhang Y. Circadian rhythm and neurodegenerative disorders. *Brain Science Advances.* 2020;6(2): 71-80
16. Comella, C.L. (2007), Sleep disorders in Parkinson's disease: An overview. *Mov. Disord.*, 22: S367-S373.
17. Videnovic A, Noble C, Reid KJ, et al. Circadian Melatonin Rhythm and Excessive Daytime Sleepiness in Parkinson Disease. *JAMA Neurol.* 2014;71(4):463–469.
18. Balestrino, R. and Schapira, A. (2020), Parkinson disease. *Eur J Neurol*, 27: 27-42.
19. Tekriwal A, Kern DS, Tsai J, et al REM sleep behaviour disorder: prodromal and mechanistic insights for Parkinson's disease *Journal of Neurology, Neurosurgery & Psychiatry* 2017;**88**:445-451.
20. Tarianyk K, Shkodina A, Lytvynenko N. CIRCADIAN RHYTHM DISORDERS AND NON-MOTOR SYMPTOMS IN DIFFERENT MOTOR SUBTYPES OF PARKINSON'S DISEASE. *Georgian Med News.* 2021;(320):100-106.
21. Parkinson Progression Marker Initiative. The Parkinson Progression Marker Initiative (PPMI). *Prog Neurobiol.* 2011;95(4):629-635.
22. Michal Rafal Zareba, Magdalena Fafrowicz, Tadeusz Marek, Ewa Beldzik, Halszka Oginska & Aleksandra Domagalik (2022) Late chronotype is linked to greater cortical thickness in the left fusiform and entorhinal gyri, *Biological Rhythm Research*, 53:10, 1626-1638.
23. Halszka Ogińska, Can you feel the rhythm? A short questionnaire to describe two dimensions of chronotype, *Personality and Individual Differences*, Volume 50, Issue 7, 2011, Pages 1039-1043,

24. Oginska H, Mojsa-Kaja J, Mairesse O. Chronotype description: In search of a solid subjective amplitude scale. *Chronobiol Int*. 2017;34(10):1388-1400.
25. Murray W. Johns, A New Method for Measuring Daytime Sleepiness: The Epworth Sleepiness Scale, *Sleep*, Volume 14, Issue 6, November 1991, Pages 540–545
26. Daniel J. Buysse, Charles F. Reynolds, Timothy H. Monk, Susan R. Berman, David J. Kupfer, The Pittsburgh sleep quality index: A new instrument for psychiatric practice and research, *Psychiatry Research*, Volume 28, Issue 2, 1989, Pages 193-213,
27. <https://www.fil.ion.ucl.ac.uk/~john/misc/VBMclass15.pdf>
28. J. Sui, H. He, G. D. Pearlson, T. Adali, K. A. Kiehl, Q. Yu, V.P. Clark, E. Castro, T. White, B. A. Mueller, B. C. Ho, N. C. Andreasen, V .D. Calhoun, "Three-way (N-way) fusion of brain imaging data based on mCCA+jICA and its application to discriminating schizophrenia", *Neuroimage* 2, 119-132, 2013.
29. Cullell N, Cárcel-Márquez J, Gallego-Fábrega C, et al. Sleep/wake cycle alterations as a cause of neurodegenerative diseases: A Mendelian randomization study. *Neurobiology of Aging*. 2021;106:320.e1-320.e12. doi:<https://doi.org/10.1016/j.neurobiolaging.2021.05.008>
30. Marano M, Rosati J, Magliozzi A, et al. Circadian profile, daytime activity, and the Parkinson's phenotype: A motion sensor pilot study with neurobiological underpinnings. *Neurobiology of Sleep and Circadian Rhythms*. 2023;14:100094-100094. doi:<https://doi.org/10.1016/j.nbscr.2023.100094>
31. Pagano G, Niccolini F, Politis M. Imaging in Parkinson's disease. *Clin Med (Lond)*. 2016;16(4):371-375. doi:10.7861/clinmedicine.16-4-371
32. Righini A, Antonini A, Ferrarini M, et al. Thin section MR study of the basal ganglia in the differential diagnosis between striatonigral degeneration and Parkinson disease. *J Comput Assist Tomogr*. 2002;26(2):266-271. doi:10.1097/00004728-200203000-00018
33. Ramírez VM, Forbes F, Coupé P, Dojat M. No Structural Differences Are Revealed by VBM in 'De Novo' Parkinsonian Patients. *Stud Health Technol Inform*. 2019;264:268-272. doi:10.3233/SHTI190225

34. Heim B, Krismer F, De Marzi R, Seppi K. Magnetic resonance imaging for the diagnosis of Parkinson's disease. *J Neural Transm (Vienna)*. 2017;124(8):915-964. doi:10.1007/s00702-017-1717-8
35. Blair JC, Barrett MJ, Patrie J, et al. Brain MRI Reveals Ascending Atrophy in Parkinson's Disease Across Severity. *Frontiers in Neurology*. 2019;10. doi:https://doi.org/10.3389/fneur.2019.01329
36. Long D, Wang J, Xuan M, et al. Automatic classification of early Parkinson's disease with multi-modal MR imaging. *PLoS One*. 2012;7(11):e47714. doi:10.1371/journal.pone.0047714
37. Xu L, Groth KM, Pearlson G, Schretlen DJ, Calhoun VD. Source-based morphometry: the use of independent component analysis to identify gray matter differences with application to schizophrenia. *Hum Brain Mapp*. 2009;30(3):711-724. doi:10.1002/hbm.20540
38. C. Scarpazza, S. Tognin, S. Frisciata, G. Sartori, and A. Mechelli, "False positive rates in Voxel-based Morphometry studies of the human brain: Should we be worried?," *Neurosci. Biobehav. Rev.*, vol. 52, pp.49–55, May 2015